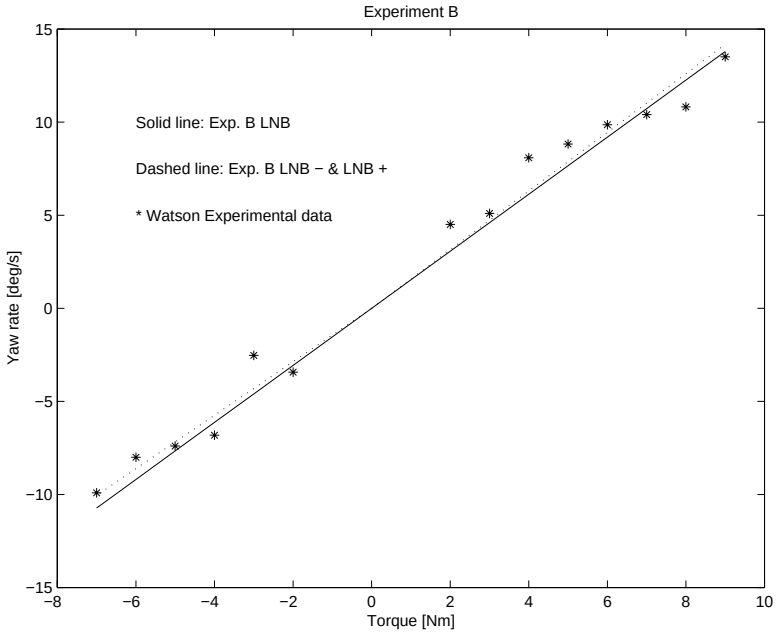

4.22.Yaw rate as a function of applied torque: experiment B, Watson data

a consequence the following *eta-models* are tested and identified:

$$\eta\text{LNB} \quad : \quad \begin{bmatrix} \tau_+ \\ \vdots \\ 0 \end{bmatrix} = \begin{bmatrix} \dot{\psi}_+ & 0 \\ \vdots & \vdots \\ \dot{\psi}_- & -\tau_- \end{bmatrix} \begin{bmatrix} k_r \\ \eta \end{bmatrix} \tag{4.19}$$

$$\eta\text{LB} \quad : \quad \begin{bmatrix} \tau_+ \\ \vdots \\ 0 \end{bmatrix} = \begin{bmatrix} \dot{\psi}_+ & 1 & 0 \\ \vdots & \vdots & \vdots \\ \dot{\psi}_- & 1 & -\tau_- \end{bmatrix} \begin{bmatrix} k_r \\ b \\ \eta \end{bmatrix} \tag{4.20}$$

$$\eta\text{LQNB} \quad : \quad \begin{bmatrix} \tau_+ \\ \vdots \\ 0 \end{bmatrix} = \begin{bmatrix} \dot{\psi}_+ & \dot{\psi}_+|\dot{\psi}_+| & 0 \\ \vdots & \vdots & \vdots \\ \dot{\psi}_- & \dot{\psi}_-|\dot{\psi}_-| & -\tau_- \end{bmatrix} \begin{bmatrix} k_r \\ k_{r|r|} \\ \eta \end{bmatrix} \tag{4.21}$$

$$\eta\text{LQB} \quad : \quad \begin{bmatrix} \tau_+ \\ \vdots \\ 0 \end{bmatrix} = \begin{bmatrix} \dot{\psi}_+ & \dot{\psi}_+|\dot{\psi}_+| & 1 & 0 \\ \vdots & \vdots & \vdots & \vdots \\ \dot{\psi}_- & \dot{\psi}_-|\dot{\psi}_-| & 1 & -\tau_- \end{bmatrix} \begin{bmatrix} k_r \\ k_{r|r|} \\ b \\ \eta \end{bmatrix} \tag{4.22}$$

Exp. B eta-model	Watson			
Model	ηLNB	ηLB	ηLQNB	ηLQB
$k_r\ [Nms/rad]$	36.11	39.23	24.79	27.13
$k_{r\|r\|}\ [Nms^2/rad^2]$	-	-	62.14	57.79
$b\ [Nm]$	-	-0.54	-	-0.27
η	0.89	1.07	0.82	0.92
$100\frac{\sigma_{k_r}}{\|k_r\|}[\%]$	4.29	9.51	23.12	28.38
$100\frac{\sigma_{k_{r\|r\|}}}{\|k_{r\|r\|}\|}[\%]$	-	-	49.16	57
$100\frac{\sigma_b}{\|b\|}[\%]$	-	108.8	-	209
$100\frac{\sigma_\eta}{\|\eta\|}[\%]$	8.06	19.58	8.63	22.9
$J_{LS}\ [(Nm)^2]$	6.13	5.693	4.4542	4.3545
$\nu\ DOF$	12	11	11	10

Exp. B eta-mod	Kvh			
Model	ηLNB	ηLB	ηLQNB	ηLQB
$k_r\ [Nms/rad]$	33.66	38.19	23.08	27.84
$k_{r\|r\|}\ [Nms^2/rad^2]$	-	-	54.07	43.98
$b\ [Nm]$	-	-0.83	-	-0.51
η	0.8	1.07	0.73	0.91
$100\frac{\sigma_{k_r}}{\|k_r\|}[\%]$	4.29	9.01	24.89	28.95
$100\frac{\sigma_{k_{r\|r\|}}}{\|k_{r\|r\|}\|}[\%]$	-	-	52.85	71.08
$100\frac{\sigma_b}{\|b\|}[\%]$	-	69.7	-	117.13
$100\frac{\sigma_\eta}{\|\eta\|}[\%]$	8.70	18.57	10.22	24.59
$J_{LS}\ [(Nm)^2]$	6.1242	5.159	4.6204	4.3066
$\nu\ DOF$	12	11	11	10

The $\hat{\eta} < 1$ value of the η estimate and its very low value of the relative percentile error shows both, that the expected efficiency loss actually takes place, and that it can be correctly modeled by the η parameter. Moreover the simple ηLNB model is confirmed again to be the best one as both the bias and quadratic drag relative errors given by the other models are very large. When experiment A is considered also propeller-propeller interactions among the thrusters on the same vehicle side, i.e. FL-RL and FR-RR, should be also taken into account. As it is not feasible to distinguish, in this case, between the loss of efficiency due to propeller-hull and propeller-propeller interactions, they are modeled by a unique parameter as follows. From the above experimental results and the consequent discussion, the most reliable model is the simple LNB one. Moreover, with reference to the above tables, comparing the residual least squares cost J_{LS} (4.4) of the experiment B LNB model ($J_{LS} = 10.3(Nm)^2$ for the Kvh data and $J_{LS} = 7.36(Nm)^2$ for the Watson data) with the experiment B ηLNB one ($J_{LS} = 6.12(Nm)^2$ for the Kvh data and $J_{LS} = 6.13(Nm)^2$ for the Watson data), the ηLNB model guarantees the best performance. Intuitively the ηLNB model estimate of k_r is the most reliable as the torque values adopted in the ηLNB model are the closest to the thrust tunnel identified ones. Consequently an efficiency parameter modeling both the propeller propeller and propeller hull interactions occurring in experiment A can be introduced as:

$$\eta_A \tau_A = \hat{k}_r \dot{\psi} \tag{4.23}$$

being $\hat{k}_r$ the linear drag ηLNB model estimate, η_A the experiment A efficiency parameter to be identified and τ_A the thrust tunnel model experiment A torque. From the above tables it follows that the $\hat{k}_r$ linear drag ηLNB model estimate is

$$\begin{aligned} \hat{k}_r &= 36.11\ Nms/rad : Watson \\ \hat{k}_r &= 33.66\ Nms/rad : Kvh \end{aligned}$$

As a consequence, the LS estimate of η_A relative to equation (4.23) is:

$$Watson \;:\; \eta_A = 0.85 \pm 0.04 \Rightarrow 100\frac{\sigma_{\eta_A}}{\eta_A} = 4.7\%\ J_{LS} = 8.26Nm$$
$$Kvh \;:\; \eta_A = 0.81 \pm 0.03 \Rightarrow 100\frac{\sigma_{\eta_A}}{\eta_A} = 3.7\%\ J_{LS} = 4.38Nm$$

where the parameter errors have been calculated according to equations (4.12) and (4.6).

In conclusion the yaw motion of the ROMEO ROV vehicle in the velocity range $[-10\,\mathrm{deg}/s, 10\,\mathrm{deg}/s]$ is best modeled by an ηLNB model having a linear drag parameter $k_r = 34 \pm 2\ Nms/rad$ (KVH value). Moreover the above results have shown that modeling the left hand side and right hand side turns with different models is unnecessary and that the propeller hull and propeller propeller interactions may reduce the ideal thruster efficiency of about 15% or 20%.

4.2.6 Surge model identification

The considered surge model is the same simplified uncoupled one (4.13) adopted for the other degrees of freedom, i.e.

$$m_u\dot{u} = -k_u u - k_{u|u|}u|u| + \tau_u + \varepsilon \tag{4.24}$$

The experimental data used to identify this model consists in the applied voltage on the four horizontal thrusters and the vehicles position with respect to the swimming pool wall as measured by a $3.3Hz$ sampling rate sonar profiler. In order to identify the drag coefficients a constant force has been applied to the vehicle and the corresponding regime value of the surge velocity has been estimated fitting by least squares the position measurements. Moreover, to evaluate the loss of efficiency in the surge direction due to propeller propeller and propeller hull interactions, the input force has been applied with three different thrust mappings denoted in the following by A, B and C: with reference to figures (4.1), (4.2), (4.3) the three type of experiments consist in

A Only the front thrusters are used: their efficiency, with respect to the thrust tunnel identified model, is assumed to be 100% when pushing forward and eventually less when pushing backwards due to interference between the thruster outgoing water flow and the vehicles hull.

B All the 4 thrusters are used: their efficiency, with respect to the thrust tunnel identified model, is assumed to be eventually reduced by the interference of the front and rear thruster water flows between each other and with the vehicles hull.

C Only the rear thrusters are used: their efficiency, with respect to the thrust tunnel identified model, is assumed to be 100% when pushing backwards (negative x direction) and eventually less when pushing forward due to interference between the thruster outgoing water flow and the vehicles hull.

The underlying idea is that when the front thrusters push backwards or the rear one

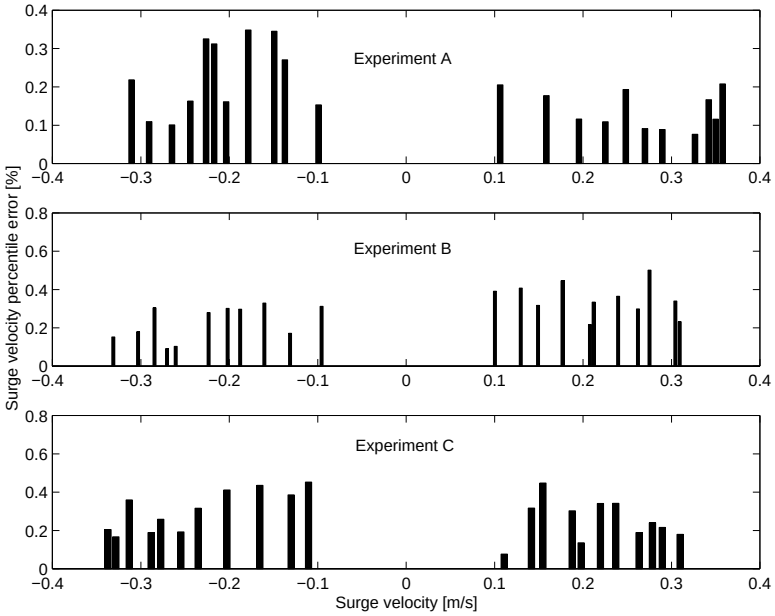

4.23.Surge velocity percentile relative error for experiments A, B and C

push forward, their efficiency may be affected by a propeller hull interaction due to the fact that in such circumstances the outgoing water flow is directed towards the vehicle. Moreover when all 4 thruster operate in the surge direction the outgoing and ingoing flows of the front and rear thrusters may be affected by the presence of each other thus giving rise to a propeller propeller interaction. The estimated velocity for each of the three kind of experiments is very precise as shown in figure (4.23). The relative percentile errors displayed in figure (4.23) have been calculated as $100\hat{\sigma}_{\hat{u}}/\hat{u}$ being $\hat{u}$ the least squares estimate of the surge velocity and $\hat{\sigma}_{\hat{u}}$ its estimated standard deviation as given by the application of equations (4.5), (4.6), (4.12) to the kinematic model

$$\begin{aligned} x &= ut + \varepsilon \\ x &: \text{ sonar measurements} \end{aligned}$$

The *nominal* applied surge forces[4] range from $10N$ to $60N$. Indicating with u_{A+}, u_{B+}, u_{C+}, u_{A-}, u_{B-}, u_{C-}, τ_{A+}, τ_{B+}, τ_{C+}, τ_{A-}, τ_{B-} and τ_{C-} the row vectors containing the norms of each regime surge velocity and corresponding nominal applied thrusts of experiments A, B and C in the positive $(+)$ and negative $(-)$ directions, the consid-

[4] As estimated by the thrust tunnel model

ered surge models are

$$\begin{bmatrix} \tau_{A+} \\ 0 \end{bmatrix} = \begin{bmatrix} u_{A+} & u_{A+}|u_{A+}| & 0 \\ u_{C+} & u_{C+}|u_{C+}| & -\tau_{C+} \end{bmatrix} \begin{bmatrix} k_u^+ \\ k_{u|u|}^+ \\ \eta_u^+ \end{bmatrix} \tag{4.25}$$

$$\begin{bmatrix} \tau_{C-} \\ 0 \end{bmatrix} = \begin{bmatrix} u_{C-} & u_{C-}|u_{C-}| & 0 \\ u_{A-} & u_{A-}|u_{A-}| & -\tau_{A-} \end{bmatrix} \begin{bmatrix} k_u^- \\ k_{u|u|}^- \\ \eta_u^- \end{bmatrix} \tag{4.26}$$

$$\begin{bmatrix} \tau_{A+} \\ \tau_{C-} \\ 0 \\ 0 \end{bmatrix} = \begin{bmatrix} u_{A+} & u_{A+}|u_{A+}| & 0 \\ u_{C-} & u_{C-}|u_{C-}| & 0 \\ u_{A-} & u_{A-}|u_{A-}| & -\tau_{A-} \\ u_{C+} & u_{C+}|u_{C+}| & -\tau_{C+} \end{bmatrix} \begin{bmatrix} k_u \\ k_{u|u|} \\ \eta_u \end{bmatrix} \tag{4.27}$$

being (4.25) relative to the forward direction drag coefficients and the rear thrusters propeller hull interaction efficiency coefficient, (4.26) relative to the backward direction drag coefficients and the front thrusters propeller hull interaction efficiency coefficient and (4.27) relative to a model that does not distinguish the positive and negative directions. Each u and τ vector in the above equations (4.25), (4.26), (4.27) has dimension 11×1. Applying the least squares technique to the three models (4.25), (4.26) and (4.27) yields

$$\begin{array}{lll} k_u^+ = (38 \pm 7) Ns/m & k_{u|u|}^+ = (333 \pm 24) Ns^2/m^2 & \eta_u^+ = (0.72 \pm 0.02) \\ k_u^- = (53 \pm 7) Ns/m & k_{u|u|}^- = (347 \pm 24) Ns^2/m^2 & \eta_u^- = (0.80 \pm 0.02) \\ k_u = (50 \pm 8) Ns/m & k_{u|u|} = (322 \pm 26) Ns^2/m^2 & \eta_u = (0.76 \pm 0.02) \end{array}$$

where the parameter errors are the standard deviations as calculated by equations (4.6) and (4.12). To evaluate the performance of the considered models the residual cost $J_{LS}(\hat{\boldsymbol{\theta}})$ (4.4) and the relative degrees ν of freedom are reported:

$$\begin{array}{lll} J_{LS}^+ = 54.33N^2 & \nu^+ = 22 - 3 = 19 & \frac{J_{LS}^+}{\nu^+} = 2.86N^2 \\ J_{LS}^- = 45.16N^2 & \nu^- = 22 - 3 = 19 & \frac{J_{LS}^-}{\nu^-} = 2.37N^2 \\ J_{LS} = 241.17N^2 & \nu = 44 - 3 = 41 & \frac{J_{LS}}{\nu} = 5.88N^2 \end{array}$$

showing that in the considered thrust and velocity ranges the best performance is achieved distinguishing two different models for the forward and backward motion which is not surprising in consideration of the open frame structure of the vehicle shown in figure (4.1) and (4.2). For a qualitative evaluation of the reliability of the proposed model refer to figure (4.24) where the experimental data of the C experiment is fitted by

$$\begin{aligned} \tau_{C-} &= k_u^- u_{C-} + k_{u|u|}^- u_{C-}|u_{C-}| : \mathbf{u}^T \mathbf{e}_x < 0 \\ \eta_u^+ \tau_{C+} &= k_u^+ u_{C+} + k_{u|u|}^+ u_{C+}|u_{C+}| : \mathbf{u}^T \mathbf{e}_x \geq 0 \end{aligned}$$

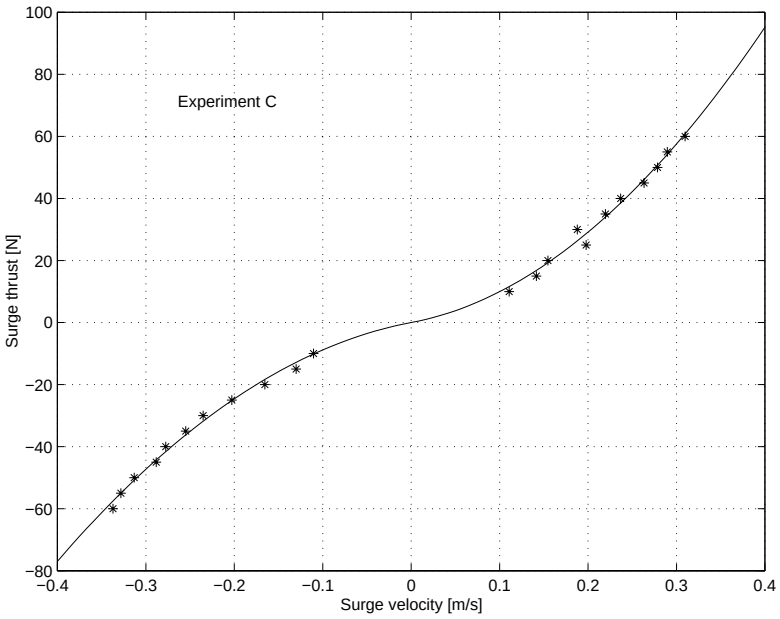

4.24.Experiment C fitted data.

Finally the loss of efficiency related to the propeller propeller and propeller hull interactions occurring when all four thrusters are adopted for a forward motion has been estimated with the data of experiment B: assuming the drag coefficients in the forward direction to be $k_u^+ = (38 \pm 7)Ns/m$ and $k_{u|u|}^+ = (333 \pm 24)Ns^2/m^2$ the least squares fitting of the model

$$k_u^+ u_{B+} + k_{u|u|}^+ u_{B+}|u_{B+}| = \tau_B \eta_{all}$$

yields

$$\eta_{all} = (0.75 \pm 0.01)$$

showing the relevance of the considered phenomenon. The above reported analysis refers to the vehicles configuration shown in the first 5 (from top to bottom and from left to right) pictures in figure (4.1). To evaluate the sensitivity of the drag and efficiency parameters on the vehicles payload configuration, experiments A, B and C described above have been repeated with a plankton sampling equipment mounted on ROMEO as shown in the bottom right picture in figure (4.1). Fitting these data with the models given by equations (4.25) and (4.26) yields

$$\begin{array}{lll} k_u^+ = (40 \pm 12)Ns/m & k_{u|u|}^+ = (305 \pm 38)Ns^2/m^2 & \eta_u^+ = (0.68 \pm 0.03) \\ k_u^- = (25 \pm 7)Ns/m & k_{u|u|}^- = (405 \pm 24)Ns^2/m^2 & \eta_u^- = (0.61 \pm 0.02) \end{array}$$

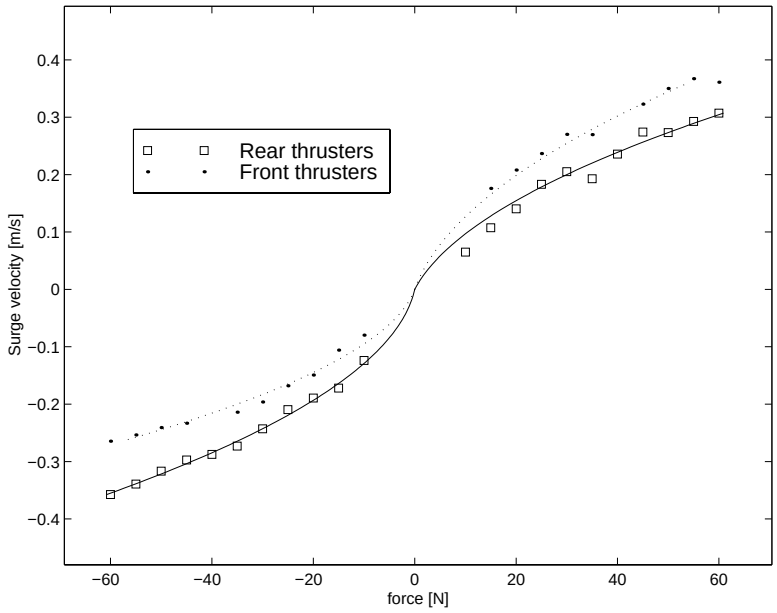

4.25.Estimated surge velocity versus the nominal, i.e. thrust tunnel model, applied force with the plankton sampling payload configuration.

and

$$J_{LS}^{+} = 109.6N^2 \quad \nu^{+} = 20 - 3 = 17 \quad \frac{J_{LS}^{+}}{\nu^{+}} = 6.4N^2$$
$$J_{LS}^{-} = 39.6N^2 \quad \nu^{-} = 21 - 3 = 18 \quad \frac{J_{LS}^{-}}{\nu^{-}} = 2.2N^2$$

showing that the considered payload indeed has an important, although not dramatic, influence of the dynamics of the vehicle. The importance of the efficiency parameter role may be better understood plotting the estimated regime velocities versus the nominal applied thruster forces relative to the experiments A (only front thrusters) and C (only rear thrusters) as shown in figure (4.25). The solid line in figure (4.25) refers to the model

$$\begin{aligned} \tau_{C-} &= k_u^{-} u_{C-} + k_{u|u|}^{-} u_{C-} |u_{C-}| : \mathbf{u}^T \mathbf{e}_x < 0 \\ \eta_u^{+} \tau_{C+} &= k_u^{+} u_{C+} + k_{u|u|}^{+} u_{C+} |u_{C+}| : \mathbf{u}^T \mathbf{e}_x \geq 0 \end{aligned}$$

and the dashed one to the model

$$\begin{aligned} \eta_u^{-} \tau_{A-} &= k_u^{-} u_{A-} + k_{u|u|}^{-} u_{A-} |u_{A-}| : \mathbf{u}^T \mathbf{e}_x < 0 \\ \tau_{A+} &= k_u^{+} u_{A+} + k_{u|u|}^{+} u_{A+} |u_{C+}| : \mathbf{u}^T \mathbf{e}_x \geq 0 \end{aligned}$$

4.2.7 Sway model identification

The considered sway axis model is

$$m\dot{v} = k_v v + k_{v|v|} v|v| + \tau_v + \varepsilon$$

in accordance with equation (4.13). As for the surge motion, the sway drag coefficients have been estimated by constant applied thrust in 3 different thrust mapping configurations:

A With reference to figure (4.3), only the left thrusters are used: their efficiency, with respect to the thrust tunnel identified model, is assumed to be 100% when pushing right (positive y direction) and eventually less when pushing left (negative y direction) due to interference between the thruster outgoing water flow and the vehicles hull.

B With reference to figure (4.3), only the right thrusters are used: their efficiency, with respect to the thrust tunnel identified model, is assumed to be 100% when pushing left (negative y direction) and eventually less when pushing right (positive y direction) due to interference between the thruster outgoing water flow and the vehicles hull.

C All the 4 thrusters are used: their efficiency, with respect to the thrust tunnel identified model, is assumed to be eventually reduced, in both y directions, by the interference of the left and right thruster water flows between each other and with the vehicles hull.

The measured data consists in the thruster applied voltage and the vehicles position as measured by a $3.3Hz$ sampling rate sonar profiler with respect to the swimming pool wall. The sway velocity is estimated applying least squares to the position measurements giving rise to very precise estimates (less then a 3% error) as shown by the plots in figure (4.26).

The velocity standard deviation has been calculated according to equations (4.6) and (4.12). Given these data and in accordance with the surge case, the following 3 models have been considered:

$$\begin{bmatrix} \tau_{A+} \\ 0 \end{bmatrix} = \begin{bmatrix} v_{A+} & v_{A+}|v_{A+}| & 0 \\ v_{B+} & v_{B+}|v_{B+}| & -\tau_{B+} \end{bmatrix} \begin{bmatrix} k_v^+ \\ k_{v|v|}^+ \\ \eta_v^+ \end{bmatrix} \tag{4.28}$$

$$\begin{bmatrix} \tau_{B-} \\ 0 \end{bmatrix} = \begin{bmatrix} v_{B-} & v_{B-}|v_{B-}| & 0 \\ v_{A-} & v_{A-}|v_{A-}| & -\tau_{A-} \end{bmatrix} \begin{bmatrix} k_v^- \\ k_{v|v|}^- \\ \eta_v^- \end{bmatrix} \tag{4.29}$$

$$\begin{bmatrix} \tau_{A+} \\ \tau_{B-} \\ 0 \\ 0 \end{bmatrix} = \begin{bmatrix} v_{A+} & v_{A+}|v_{A+}| & 0 \\ v_{B-} & v_{B-}|v_{B-}| & 0 \\ v_{A-} & v_{A-}|v_{A-}| & -\tau_{A-} \\ v_{B+} & v_{B+}|v_{B+}| & -\tau_{B+} \end{bmatrix} \begin{bmatrix} k_v \\ k_{v|v|} \\ \eta_v \end{bmatrix} \tag{4.30}$$

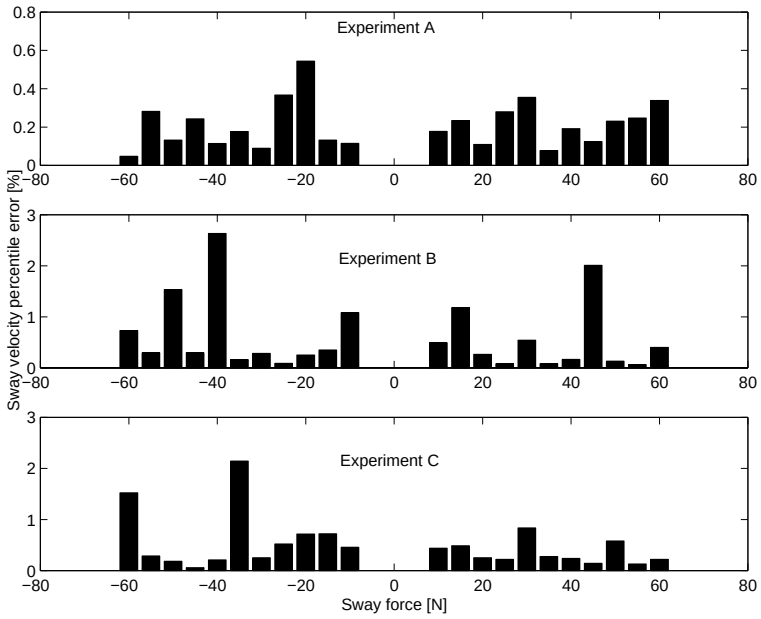

4.26.Relative percentile sway velocity error.

being τ_{A+}, τ_{A-}, v_{A+}, v_{A-}, v_{B+}, v_{B-}, τ_{B+} and τ_{B-} vectors whose components are the norms of the thrust tunnel model calculated thrust and the norms of the least squares estimated sway velocities. As the experimental data has been acquired for nominal applied thrusts of norms ranging from $10N$ to $60N$ with $5N$ increments, each of the above τ and v vector has dimension 11×1. Equations (4.28) and (4.29) assume different drag coefficients in the positive and negative y direction, while equation (4.30) assumes full symmetry with respect to the x axis. The resulting parameter vector estimates according to the three models are:

$$\begin{array}{lll} k_v^+ = (148 \pm 27)Ns/m & k_{v|v|}^+ = (302 \pm 127)Ns^2/m^2 & \eta_v^+ = (0.87 \pm 0.05) \\ k_v^- = (104 \pm 22)Ns/m & k_{v|v|}^- = (735 \pm 121)Ns^2/m^2 & \eta_v^- = (0.95 \pm 0.04) \\ k_v = (150 \pm 20)Ns/m & k_{v|v|} = (363 \pm 101)Ns^2/m^2 & \eta_v = (0.90 \pm 0.04) \end{array}$$

and the residual least squares cost $J_{LS}(\hat{\boldsymbol{\theta}})$ (4.4) is:

$$\begin{array}{lll} J_{LS}^+ = 370.89N^2 & \nu^+ = 22 - 3 = 19 & \frac{J_{LS}^+}{\nu^+} = 19.5N^2 \\ J_{LS}^- = 194.87N^2 & \nu^- = 22 - 3 = 19 & \frac{J_{LS}^-}{\nu^-} = 10.26N^2 \\ J_{LS} = 877.6N^2 & \nu = 44 - 3 = 41 & \frac{J_{LS}}{\nu} = 21.4N^2 \end{array}$$

The performance of these models can be graphically evaluated by the plots of the experiment A and B data fitted as follows:

$$\begin{aligned} \tau_A &= k_v^+ v + k_{v|v|}^+ v|v| : \boldsymbol{\tau}_A^T \mathbf{e}_y > 0 \\ \eta_v^- \tau_A &= k_v^- v + k_{v|v|}^- v|v| : \boldsymbol{\tau}_A^T \mathbf{e}_y < 0 \end{aligned}$$

in figure (4.27),

$$\begin{aligned} \tau_B &= k_v^- v + k_{v|v|}^- v|v| : \boldsymbol{\tau}_B^T \mathbf{e}_y < 0 \\ \eta_v^+ \tau_B &= k_v^+ v + k_{v|v|}^+ v|v| : \boldsymbol{\tau}_B^T \mathbf{e}_y > 0 \end{aligned}$$

in figure (4.28). As far as the experiment C (all four thrusters) is concerned, its data can be fitted with a model that takes into account the propeller propeller and propeller hull interactions of the horizontal thrusters, and assumes the drag coefficients in the two directions to be k_v^+, $k_{v|v|}^+$, k_v^- and $k_{v|v|}^-$ previously identified by experiment A (only left thrusters) and B (only right thrusters) as described above. In particular the following is considered:

$$\eta_C^+ \tau_{C+} = k_v^+ v + k_{v|v|}^+ v|v| : \boldsymbol{\tau}_C^T \mathbf{e}_y > 0 \quad (4.31)$$

$$\eta_C^- \tau_{C-} = k_v^- v + k_{v|v|}^- v|v| : \boldsymbol{\tau}_C^T \mathbf{e}_y < 0 \quad (4.32)$$

and with the usual least squares technique the efficiency parameters η_C^+ and η_C^- are found

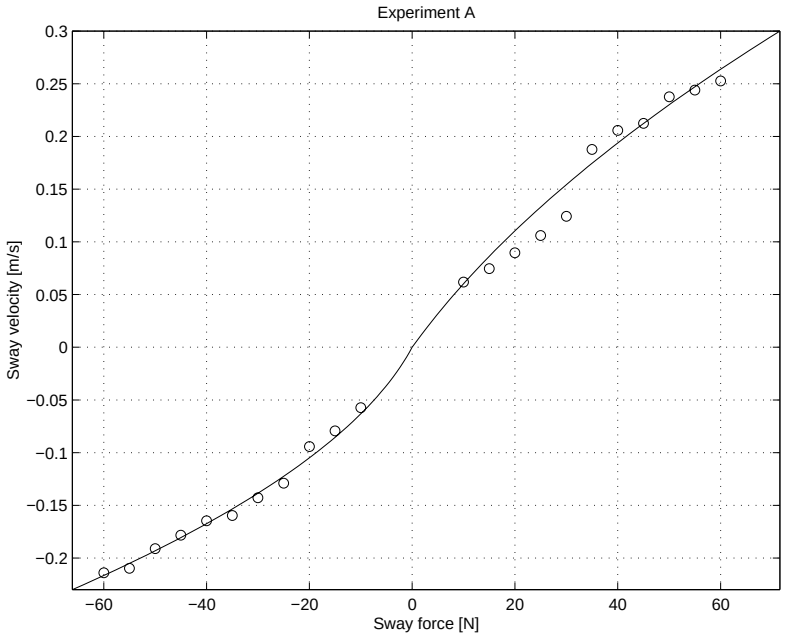

4.27.Experiment A fitted data.

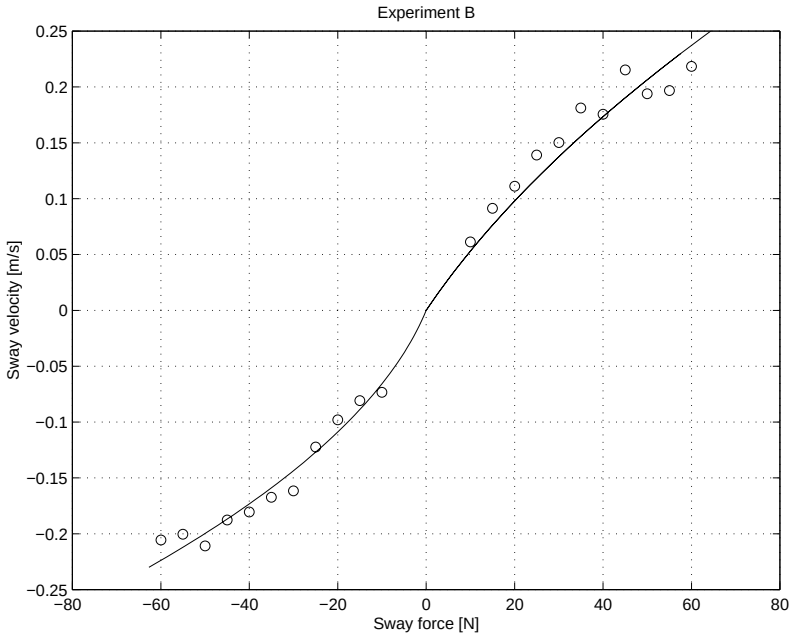

4.28.Experiment B fitted data.

to be:

$$\begin{aligned} \eta_C^+ &= (0.78 \pm 0.02) \\ \eta_C^- &= (0.76 \pm 0.03) \end{aligned}$$

The performance of the model taking into account the propeller propeller and propeller hull interactions of the four thrusters as described by equations (4.31) and (4.32) is graphically shown in figure (4.29) where the model calculated sway velocity is plotted with the experimental data of experiment C.

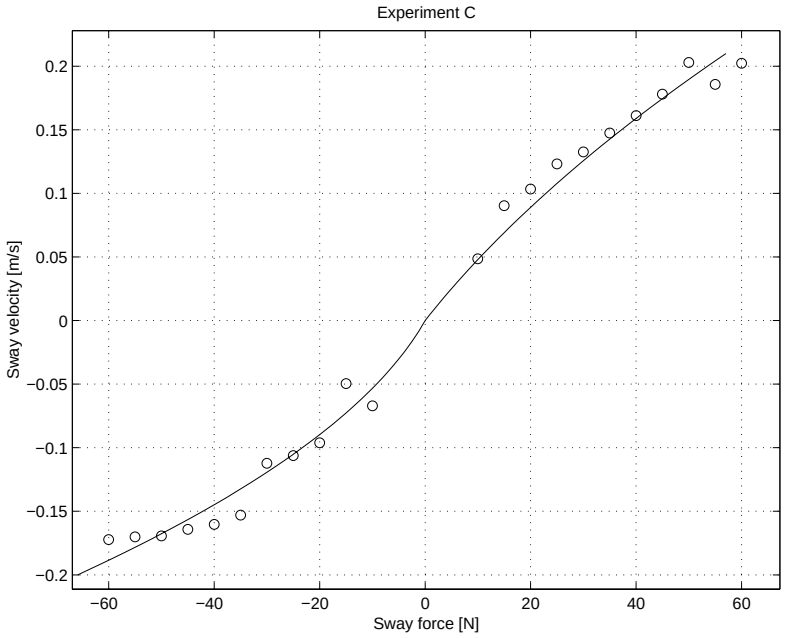

4.29.Experiment C fitted data.

4.2.8 Inertia parameters identification

An identification procedure of the inertial parameter of a decoupled model of an UUV is proposed. The main idea is to consider the drag parameters known and use this knowledge to design a sub-optimal experiment for the identification of the inertial quantities. The model to identify is given by equation (4.13) here reported for reference

$$m\dot{\xi} = -k_\xi \xi - k_{\xi|\xi|}\xi|\xi| + \eta_\xi \tau_\xi + \varepsilon \tag{4.33}$$

where m is the inertial parameter, ξ is the velocity, $\dot{\xi}$ the acceleration, τ_ξ the nomi-

nal cavitation tunnel identified force (or torque), η_ξ the propeller interaction efficiency parameter, k_ξ, $k_{\xi|\xi|}$ the linear and quadratic drag coefficients and ε the noise. τ_ξ is considered known as the propulsion system has been modeled and identified as shown in section (4.2.2). The drag and efficiency coefficients are also assumed known from the identification experiments described above. Within this framework the design of the inertia parameter identification experiment has to take into account some important constraints: due to the absence of accelerometers the identification process must be performed with the only velocity and position measurements and force estimate. Moreover the adopted propulsion model is known to be very accurate when the propellers do not suddenly change revolution direction so a second constraint on the experiment design is to keep constant τ_ξs sign during the whole experiment. Supposing ξ to be

$$\xi = \xi_0 + \Delta_\xi \sin(\omega t) \tag{4.34}$$

with ξ_0, Δ_ξ constants and $\Delta_\xi << \xi_0$ equation (4.33) can be linearized to

$$m\,\dot{\xi} = \tilde{\tau}_\xi - k_l\,\xi \tag{4.35}$$

being $k_l = k_\xi + 2|\xi_0|\ k_{\xi|\xi|}$ and $\tilde{\tau}_\xi = \eta_\xi \tau_\xi + k_{\xi|\xi|}|\xi_0|\xi_0$. Equation (4.35) corresponds to a first order system

$$V(s) = \frac{k_l^{-1}}{\tau s + 1}\,(F(s) + m\xi_0) \tag{4.36}$$

with time constant

$$\tau = m/k_l = \frac{m}{k_\xi + 2|\xi_0|\ k_{\xi|\xi|}}. \tag{4.37}$$

The linear system (4.36) will have an output as equation (4.34) if the input $\tilde{\tau}_\xi$ is the sum of a constant and a sinusoidal wave of frequency ω. Notice that as m is the sum of inertia (known) and added mass (always positive) and k_ξ, $k_{\xi|\xi|}$, ξ_0 are known, a lower bound of the time constant τ is known. Moreover as added mass is expected to be at most 100% of the inertial mass, also an upper bound of τ is given. This estimate can be very useful to choose the exiting frequency ω of the input force. A common criterion [58] [56] for choice of the inputs is to maximize the cost function

$$J = -\log\det M \tag{4.38}$$

being M Fisher's information matrix which depends on the adopted inputs. In robotic applications this criterion (*d-optimal criterion*) has been successfully adopted by Swevers et al. [71] [72] for the identification of an industrial arm. Classical identification theory [56] states that a first order system as (4.36) can be optimally identified (according to criterion (4.38)) with a single sine input of frequency

$$\omega_{opt} = \frac{1}{\sqrt{3}\tau}. \tag{4.39}$$

The input force for the inertia identification experiments is thus chosen to be of the

form:

$$f(t) = f_0 + \Delta_f \sin(\omega_{opt} t) \tag{4.40}$$

The f_0 constant is selected so that its corresponding regime velocity ξ_0 is in the standard operating range, Δ_f is selected to be $\Delta_f \leq f_0$ so that force inversions are avoided and the d-optimal frequency ω_{opt} is selected in accordance to equation (4.39). The system time constant τ needed to compute ω_{opt} is *a priori* estimated by equation (4.37) as the drag coefficients are known and m is supposed to be equal to the inertia in air m_{air} plus a term ranging from 10% to 100% of m_{air} that models added mass. The output $\xi(t)$ of the linear system (4.35) with input $\tilde{\tau}_\xi = f(t)$ given by equation (4.40) is reported for reference:

$$\xi(t) = \xi_0 e^{-t/\tau} + \frac{f_0}{k_l}\left(1 - e^{-t/\tau}\right) + \frac{\Delta_f}{k_l}\frac{\sin(\omega_{opt} t) - \omega_{opt}\tau(\cos(\omega_{opt} t) - 1)}{1 + \omega_{opt}^2 \tau^2}$$

being τ given by equation (4.37).

To cope with the absence of an acceleration measurement, equation (4.13) must be integrated giving

$$m\,\xi(t) - m\,\xi_0 = \varphi(t) - k_\xi\,(\zeta(t) - \zeta_0) - k_{\xi|\xi|}\,I(t) + bt \tag{4.41}$$

$$m\,\xi(t) - m\,\xi_0 - k_\xi \zeta_0 - bt = y$$

$$y \triangleq \varphi(t) - k_\xi\,\zeta(t) - k_{\xi|\xi|}\,I(t) \tag{4.42}$$

being $\varphi(t) = \int_0^t \tau_\xi(\psi) d\psi$, $\zeta(t)$ the position, $I(t) = \int_0^t \xi(\psi)|\xi(\psi)| d\psi$, and b an eventual bias due to the mean of ε and to the numerical integrations performed to calculate φ and I. Notice that the integration process does not affect the d-optimal frequency choice as the integral of equation (4.35) has its same structure, in particular the same time constant. As the drag constants, velocity and position are known equation (4.41) can be written in discrete-time regression form $y = H\boldsymbol{\theta}$ being

$$y = \begin{bmatrix} \varphi_1 - k_\xi \zeta_1 - k_{\xi|\xi|} I_1 \\ \varphi_2 - k_\xi \zeta_2 - k_{\xi|\xi|} I_2 \\ \vdots \\ \varphi_N - k_\xi \zeta_N - k_{\xi|\xi|} I_N \end{bmatrix} \tag{4.43}$$

$$H = \begin{bmatrix} \xi_1 & -1 & -t_1 \\ \xi_2 & -1 & -t_2 \\ \vdots & \vdots & \vdots \\ \xi_N & -1 & -t_N \end{bmatrix} \tag{4.44}$$

$$\boldsymbol{\theta} = [m, (m\,\xi_0 + k_\xi \zeta_0), b]^T \tag{4.45}$$

and N the number of samples. Notice that the linearized system frequency related to equation (4.37) for the translational DOFs is below the Nyquist frequency ($1.65 Hz$)

relative to the slowest on-board sensors ($3.3Hz$ for sonars). For surge $k_u \simeq 38Ns/m$, $k_{u|u|} \simeq 333Ns^2/m^2$ assuming $m \simeq 675Kg$ and $u_0 = 0.2\ m/s$, $\nu = 1/\tau = k_l/m = \frac{k_u + 2u_0\ k_{u|u|}}{m} = 0.25Hz$.

Within this approach the uncertainty on the inertia parameter estimate is expected to be at least of the same order of magnitude of the drag parameter uncertainty. As estimating the inertia m is somehow equivalent to estimating the systems time constant $\tau = m/k_l$, by standard error analysis it follows that $\delta\tau/\tau = \delta k_l/k_l \approx 10\%$. Moreover the applied force τ_ξ, assumed to be known perfectly, will be actually affected by some error that must be reasonable thought to be of about 10%. Numerical errors will be also introduced in the computation of y as due to the absence of a velocity measurement the I quantity is calculated filtering the acquired position signal with an off line Savitzky-Golay polynomial filter to evaluate the velocity ξ and then integrating numerically $\xi|\xi|$ over time. Numerical integrations must be also performed on the position signal and on the applied fore in order to compute y. These considerations and the fact that the sampling rate of the position measurements is very low ($3.3Hz$ for sonars used for the linear DOFs and $10Hz$ for the yaw) suggests that the inertia parameter identification by only on board position measurements can not be expected to be very precise. Nevertheless the estimated value is generally good enough to provide reliable and useful models for modeling and control purposes.

4.2.9 Surge inertia parameter identification

The above described technique has been experimentally implemented on the surge and yaw axis of the ROMEO ROV. The surge experiments have been performed applying an input force as the one given by equation (4.40) with the only front thrusters: with reference to figure (4.3) and to section (4.2.6) this means that the drag coefficients are assumed to be $k_u = (38 \pm 7)Ns/m$, $k_{u|u|} = (333 \pm 24)Ns^2/m^2$ and the efficiency parameter 1. The results of three different experiments labeled SUI1 (SUrge Inertia), SUI2 and SUI3 are reported. In accordance with the input design criteria described in the previous section the applied force, in $Newton$, in each experiments is:

$$f_u = 35 + 25\sin(\frac{2\pi t}{T})$$

being $T = T_1 = 26.8s$, $T_2 = 40.2s$ and $T_3 = 53.6s$ in the SUI1, SUI2 and SUI3 experiments corresponding to frequencies $\upsilon_1 = 0.23Hz$, $\upsilon_2 = 0.16Hz$, $\upsilon_3 = 0.12Hz$. With reference to section (4.2.6) the regime velocity u_0 corresponding to the constant surge force $f_0 = 35N$ can be estimated to be $u_0 \approx 0.2m/s$ so that assuming the drag coefficients to be $k_u = 38Ns/m$ and $k_{u|u|} = 333Ns^2/m^2$ as stated above and the inertia $m \approx 450 + 50\%(450) = 675Kg$ equations (4.37) and (4.39) suggest an optimal input frequency $\omega_{opt} \approx 0.15Hz$. Figure (4.30) shows the data relative to the SUI1 experiment. From the top left plot in clock wise direction the following are displayed: the input force, the $3.3Hz$ sampling rate sonar profiler position measurement, the difference between

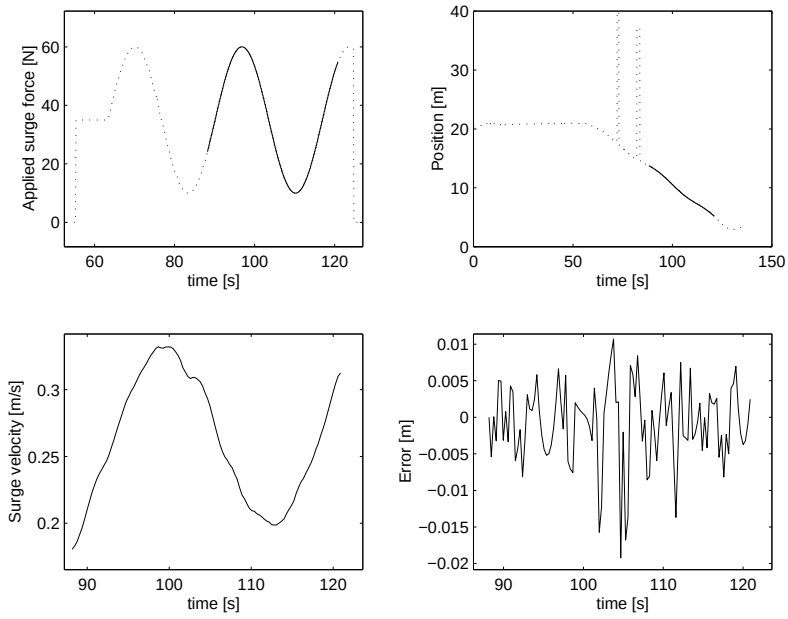

4.30.Surge inertia parameter estimation experimen. For a detailed describiton of the plots refer to the text.

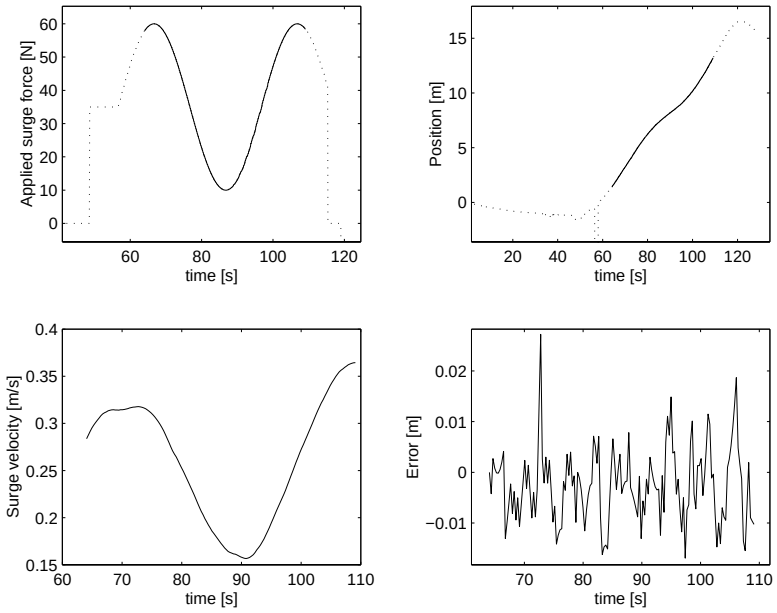

4.31.Surge inertia parameter identification experiment.

the trapezoidal rule numerical integral of the velocity signal (last plot) and the measured position and the velocity signal computed with a Savitzky-Golay off line 4^{th} order filter having a symmetrical window of 21 points. The solid curves in the position and force plots refer to the data actually adopted for the identification process while the dashed ones show the whole batch of data. Notice in the sonar measurement data the presence of two multiple echoes at the beginning of the batch. Applying the LS estimation technique outlined in the previous section to the data of the SUI1 experiment, the inertia parameter is estimated to be

$$\text{SUI1 experiment: } m = (884 \pm 55)Kg$$

being the estimation error computed on the basis of equations (4.12) and (4.6). It is worthwhile remembering that this estimation error calculation method is approximated as the measurement variance σ^2 in equation (4.6) is replaced by its estimated value given by equation (4.12). This is equivalent to the tacit assumption [68] that the fit is "good", i.e. $J_{LS}(\hat{\boldsymbol{\theta}})/\nu \approx 1$ being ν the number of degrees of freedom of the fit. In the present situation the fit is actually quite poor as $J_{LS}(\hat{\boldsymbol{\theta}})/\nu = 687N^2s^2$. As a consequence, and on the basis of the considerations developed in the previous section, the above reported inertia parameter estimation error must be underestimated. This is also confirmed by the scattered values of m obtained processing the data of experiments SUI2 and SUI3:

$$\text{SUI2 experiment} \quad : \quad m = (554 \pm 31)Kg$$

$$\text{SUI3 experiment} \quad : \quad m = (632 \pm 39)Kg$$

and by the large values of the residual costs $J_{LS}(\hat{\boldsymbol{\theta}})/\nu = 676N^2s^2$ (SUI2) and $J_{LS}(\hat{\boldsymbol{\theta}})/\nu = 1032N^2s^2$ (SUI3). Figure (4.31) shows the data relative to the SUI2 experiment. From the top left plot in clock wise direction the following are displayed: the nominal input force, the $3.3Hz$ sampling rate sonar profiler position measurement, the difference between the trapezoidal rule numerical integral of the velocity signal (shown in the last plot) and the measured position and the velocity signal computed with a Savitzky-Golay off line 4^{th} order filter having a symmetrical window of 41 points. The solid curves in the position and force plots refer to the data actually adopted for the identification process while the dashed ones show the whole batch of data.

As pointed out in the previous section the proposed methodology for ROVs inertia parameter identification is very simple, low cost, reasonably fast and based only on standard on board sensors: the major drawback being a relatively large estimation error. Nevertheless as standard ROV manoeuvres are performed with very limited accelerations, the above estimated values of the inertia parameters, although affected by an apparently large estimation error, can be successfully adopted to model the system for filtering and control purposes. To quantitatively evaluate the reliability of the estimated surge model the position measurement data of experiments SUI1 and SUI2 has been compared with the model predicted position relative to the same input forces. In figure (4.32) the position measurement of experiment SUI1 has been plotted with the position predicted by two models having inertias $m = 550\,Kg$ and $m = 860\,Kg$ and the drag coefficients fixed to their nominal values $k_u = 38Ns/m$ and $k_{u|u|} = 333Ns^2/m^2$. while in figure (4.33) the position measurement of experiment SUI2 has been plotted with the position predicted by two models having inertias $m = 705Kg$ ($\sim$ mean of $550Kg$ and $860\,Kg$) and drag coefficients $k_u = 38Ns/m$, $k_{u|u|} = 333Ns^2/m^2$ and $k_u = (38 + 7)Ns/m$, $k_{u|u|} = (333 + 24)Ns^2/m^2$. The position error between the model and the experimental data is remarkably small during the whole length of the trials for both experiments.

4.2.10 Yaw inertia parameter identification

In order to implement the above described methodology for the yaw axis the system time constant τ must be a priori estimated to compute the input torque frequency ω_{opt}. As described in section (4.2.5), the yaw model in the standard yaw rate operating range is linear. Moreover the yaw inertia identification experiments have been performed applying the input torque with a thruster mapping having unit efficiency, i.e., with reference to figure (4.3), the front left (FL) and rear right (RR) thrusters have been used for positive torques and the front right (FR) and rear left (RL) ones have been used for negative torques. As a consequence the considered yaw model is

$$I_z\dot{r} = f - k_r r \tag{4.46}$$